Subsurface Object Sensing With a Multifrequency Microwave Radiometer

Joel T. Johnson, *Member, IEEE*, Hyunjun Kim, *Student Member, IEEE*, David R. Wiggins, and Yonghun Cheon

***Abstract*—Experimental results are reported for sensing of subsurface objects with a multifrequency radiometer (MFRAD) system. Properties of the MFRAD system are reviewed, and the calibration and experimental procedures are discussed. Results with subsurface metallic, styrofoam, and plastic targets are then provided that demonstrate an oscillatory behavior in brightness temperatures versus frequency in the presence of a subsurface object. Measured data are also compared with a simple layered medium brightness temperature model and show reasonable agreement with predicted trends of brightness temperatures versus frequency. The oscillatory behaviors versus frequency obtained in the presence of both metallic and nonmetallic subsurface objects should prove advantageous for designing object detection procedures.**

***Index Terms*—Radiometry, subsurface sensing, thermal emission.**

I. Introduction

MICROWAVE radiometers are currently being considered as components of a multisensor "suite" for military and humanitarian demining applications [1]–[12]; detection and identification of subsurface objects is critical for these applications. While early passive demining studies initially emphasized millimeter-wave frequencies [13]–[16] due to the favorable spatial resolutions that can be obtained in "standoff" geometries, more recent studies have explored microwave frequencies to obtain greater sensitivities for deeper targets and for higher moisture content soils. Early efforts with microwave frequencies focused on laboratory demonstrations [1], including demonstrations of the potential of synthetic aperture microwave radiometry to improve spatial resolutions [2]. More recently, field tests performed with 5- [3], [4] and 10-GHz [5] systems have been documented, although no variations in brightness temperatures with frequency could be observed with the narrowband instruments employed. These tests showed moderate success at detecting subsurface objects (particularly metallic objects), but significant clutter contributions were also observed. As discused in [6], a microwave radiometer is similar to a ground-penetrating radar (GPR) for detecting subsurface objects in that attenuation in the background medium and target dielectric contrast with the background medium are important factors; however, radiometer and GPR systems will obtain differing responses to clutter factors such as surface roughness. The radiometer also remains sensitive to the basic "layered" structure of a subsurface object geometry even at oblique observation angles, while the GPR backscattering response is more sensitive to discontinuities in the medium (i.e., diffraction from finite target boundaries). It should be expected based on these factors that GPR and radiometer sensors will provide complementary information, making both useful components of a multisensor suite for demining.

Modeling studies for radiometer use in demining [6]–[10] have been reported that investigate the potential performance of passive microwave sensors for subsurface detection problems. In the simplest case, a subsurface object geometry is described simply in terms of a three-layer constant-temperature medium, so that brightness temperatures are related to the reflection coefficient of the three-layer medium. This model predicts that an oscillatory behavior versus frequency should be obtained in the presence of a subsurface object, but not in its absence, even when moderate environmental clutter is present. This oscillatory behavior is due to an interference between directly emitted noise fields and the same noise fields singly or multiply reflected at the layered medium boundaries. A multifrequency radiometer was therefore proposed [6], [10] as potentially providing improved detections through a search for oscillatory features in measured data. The model was extended to include surface roughness effects on the boundary [6], [7], temperature and soil moisture profile effects [8], and finite-sized targets [8], [9]. None of these additional factors modified the basic strategy of searching for oscillatory features versus frequency to improve object detections. Modeled finite-sized target brightness temperature deviations from no-target values were found to be well predicted by the three-layer model if its predictions were multiplied by a "beam-fill factor" that describes the fraction of the antenna pattern occupied by the subsurface object [9].

Initial subsurface object measurements with multifrequency microwave radiometers have only recently been reported [10]–[12]. The studies of [10] and [11] employ a stepped frequency system, while those of [12] use a multichannel system (i.e., multiple fixed frequencies), but in both cases, the predicted oscillatory features versus frequency in the presence of subsurface targets were observed. This paper describes further experiments performed with the radiometer system of [12] including metallic, styrofoam, and plastic subsurface objects.

Manuscript received May 3, 2002; revised September 23, 2002. This project was supported by Duke University under an award from the Army Research Office (ARO) (Office of the Secretary of Defense Multi-Disciplinary University Research Initiative on Humanitarian Demining) and by the Defense University Research Instrumentation Program (DURIP) under Office of Naval Research (ONR) sponsorship. The findings, opinions, and recommendations expressed therein are those of the authors and are not necessarily those of Duke University, ARO, or ONR.

The authors are with the Department of Electrical Engineering and ElectroScience Laboratory, 205 Dreese Laboratories, The Ohio State University, Columbus, OH 43210 USA (e-mail: johnson@ee.eng.ohio-state.edu).

Digital Object Identifier 10.1109/TGRS.2002.807753

The response of a microwave radiometer to plastic subsurface objects is of particular importance, given the increasing use of "low-metal" content mines and the difficulties these targets produce for many sensors. The radiometer used is described in Section II, and the experimental and calibration procedures are detailed in Section III. Results from the experiments are presented and compared with predictions of the three-layer model in Section IV, while Section V provides conclusions.

II. Multifrequency Radiometer

The multifrequency radiometer (MFRAD) used in these experiments was supported under a Defense University Research Instrumentation Project awarded in 2000. The initial design of MFRAD was a collaboration between The Ohio State University ElectroScience Laboratory and the Radiometrics Corporation, Boulder, CO,[1] while the detailed design and system construction were completed by Radiometrics. The system was delivered in November of 2001 and consists of a receiver assembly, power supply/thermal control module, and a laptop computer for data recording and system control. MFRAD is a standard Dicke switching, direct-detection radiometer, with 37 distinct receiver channels from 2–18 GHz. Johnson *et al.* [12] provide a list of the first 19 channel frequencies and bandwidths in the 2.1–6.5-GHz band (channel frequencies are also marked in Fig. 4); these channels are the most useful for humanitarian demining applications. Higher frequency channels to 18 GHz were included in MFRAD for other applications. Channel frequencies were chosen based on a radio-frequency-interference (RFI) survey at the ElectroScience Laboratory in the initial design phase. Channel choices include the "quiet" band allocation at 2690–2700 MHz [17], but channel frequencies otherwise are shared with other microwave systems. RFI is a major concern for radiometric systems, since man-made emissions on the same channels can completely obscure naturally emitted thermal noise. The measured data to be described were free of significant RFI contributions, indicating little change in the local RFI environment since the time of the design phase survey.

Fig. 1 is a receiver sensitivity plot for the 2.275- and 5-GHz channels using an internal noise diode source included in MFRAD. The standard deviation of measured brightnesses for a fixed integration time is observed to follow the ideal $1/\sqrt{\tau}$ proportionality for integration times τ up to approximately 1 s at 2.275 GHz but only up to approximately 300 ms for 5 GHz. Brightness standard deviations reported are obtained using the dielectric rod antenna calibration procedure described in Section III. In both cases (and in all the channels considered), brightness standard deviations of approximately 1 K or less were obtained for integration times longer than 1 s. The deviations from ideal behavior observed in Fig. 1 occur due to receiver gain variations that are not compensated for in the calibration procedure, and compromise the ability of the system to obtain improved sensitivity through longer integration periods. Thermal control of the receiver enclosure

[1]http://www.radiometrics.com

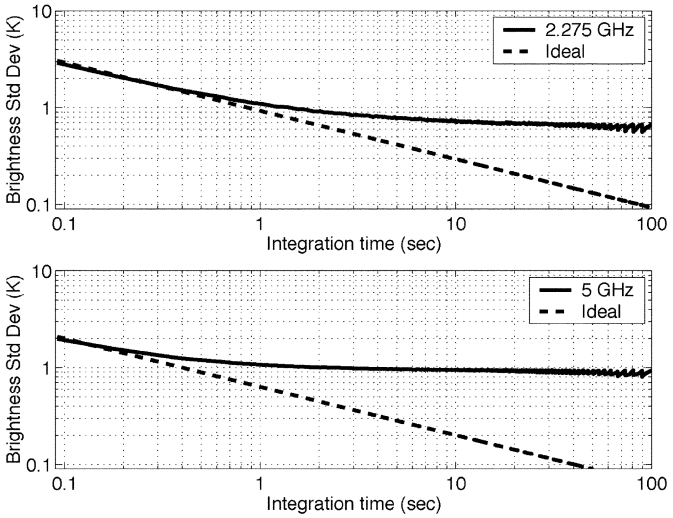

Fig. 1. Radiometer sensitivity versus integration time.

(temperature constant to within 0.1 K throughout the period of the experiments reported) reduces these effects, but the high gain of the receiver makes obtaining ideal behavior difficult for longer integration times. However, brightness standard deviations remain 1 K or less in all channels even at values of the integration time up to the time scale of hours; the entire set of measurements described in Section III was made in a 3-h period. This fact shows that receiver gain variations throughout the period of the experiment do not introduce errors significantly beyond the 1-K measurement sensitivity. Updates to the system are currently in process to improve its stability.

III. Experimental and Calibration Procedures

A series of experiments was performed in a sand-pit located in the backyard of the ElectroScience Laboratory from February to April of 2002. The data described in this paper were obtained from a single set of measurements on April 16, 2002. The goals of this set of measurements were 1) to illustrate oscillatory brightness temperatures versus frequency produced by distinct subsurface objects and 2) to demonstrate a semi-practical multifrequency radiometer system for mine detection. Several experimental factors related to the second goal will be shown to degrade the absolute accuracy of the results; however, the measurements will still be shown sufficiently accurate to achieve a reasonable illustration of oscillatory brightness variations for varying target types.

A wideband dielectric rod antenna [18]–[20] was used to allow measurements in the 2.1–6.5-GHz band of interest. While typical microwave radiometer measurements are performed in far-field observation geometries, the desire for high resolution at the ground surface motivates operation very near the ground. The rod antenna is advantageous in this case because it produces a nearly spherical wave (directional) field pattern [18] even at distances very close to the antenna, so that strong near-field effects are not observed. Results, however, remain weakly dependent on distance, so measurements made with this system, though calibrated, should be regarded as quasi

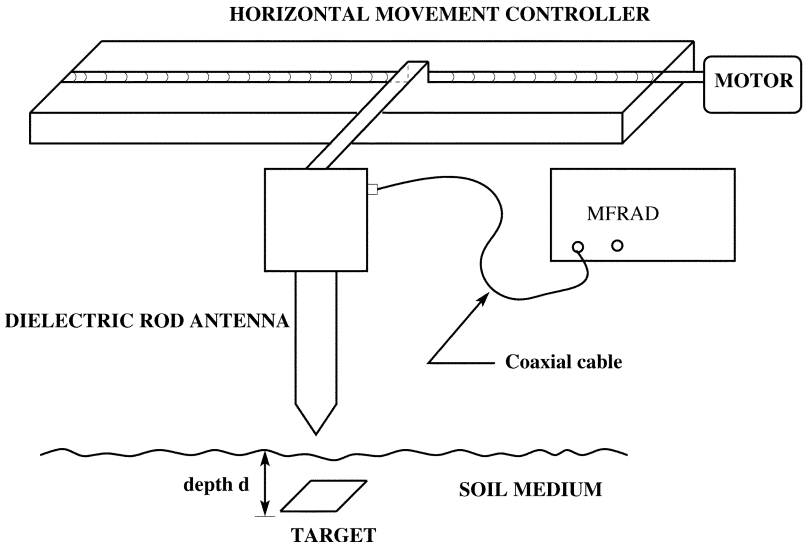

Fig. 2. Experiment setup.

brightnesses. Results in Section IV will show that measured data remain reasonably predicted by a three-layer model based on ideal far-field observing antenna patterns. The rod antenna is well matched over the frequency band of interest (S_{11} of -20 dB or less through the entire band) and is constructed of a material with negligible loss. The rod is also designed to minimize antenna and ground interactions, so that the presence of the ground and/or subsurface objects does not strongly degrade the antenna match.

Fig. 2 illustrates the measurement configuration; the rod antenna tip was located at a distance of 5.1 cm above the ground surface, and the rod was oriented to receive horizontally polarized emissions at an oblique angle of 15.75° from nadir. For this near-nadiral geometry, brightnesses in horizontal polarization should not be expected to differ significantly from those in vertical polarization, so a single polarization measurement is sufficient for this experiment. At larger observation angles, however, multiple polarization measurements could prove advantageous and are considered in the modeling study of [6]. Emissions in the third and fourth Stokes polarization parameters should be expected to be minimal for nearly azimuthally symmetric geometries as considered here, although these contributions could potentially respond to rotated subsurface objects. The utility of fully polarimetric radiometry for subsurface object detection thus remains to be explored. Antenna "spot-sizes" on the ground were estimated to be in the range of 2.5–7.5 cm in diameter through tests in which metallic targets were placed on the surface; these spot-sizes vary with frequency, and for subsurface objects they would be strongly affected by distance from the antenna and refraction in the sand medium.

Three targets were used in the experiments: a thin metallic plate of dimensions 9.2×10.2 cm, a styrofoam block of dimensions 11.7×10.2 cm with thickness 4.8 cm, and a plastic (nylon) disc target of thickness 2.5 cm and radius 3.8 cm. These targets were buried at depths from 2.5–10.2 cm in the sand; moisture content of the sand was not measured at the time of the experiments, but data analysis will be described in Section IV that retrieves a volumetric water content of approximately 1.75%. It should be expected that brightness signatures of buried targets will be related both to attenuation in the background medium and to the contrast of the target with the background medium. While the dry sand medium used minimizes attenuation problems, contrast issues remain important for the nonmetallic targets. Future experiments with other soil types and moisture contents will of course be important for assessing radiometer performance in other environments.

Measurements were made continuously as the rod antenna was translated through a 56-cm horizontal scan of approximately 8 min duration (approximately 1.8 s of available integration time per centimeter including internal calibration measurements). Results were then combined to an effective integration time of 1.65 s to reduce the measured data to approximately 61 positions per scan. The choice of 1.65 s of integration time was arbitrary, but the results to be shown in Section IV will indicate that this number of positional data provides sufficient resolution to image the subsurface objects used. Faster scan rates would also be possible without significantly degrading image properties.

A standard calibration procedure was applied for each MFRAD frequency through observations of external "hot" and "cold" load calibration targets. A flat three-layer wideband absorber was used as the "hot" load, while a similar absorber immersed in liquid nitrogen was used as the "cold" load [21]. Because the sky at these frequencies is very transmissive, it could also potentially be used as an alternate cold load to avoid use of liquid nitrogen [22]; this will be explored in future experiments. Calibration loads were placed level with the ground surface to reduce the influence of distance in the experiments. The accuracy of these calibration targets with the MFRAD system is difficult to estimate at present; however, the method proposed for detecting subsurface objects (i.e., searching for oscillatory patterns in brightness temperatures versus frequency) does not necessarily require a high absolute accuracy so long as a reasonable relative accuracy between

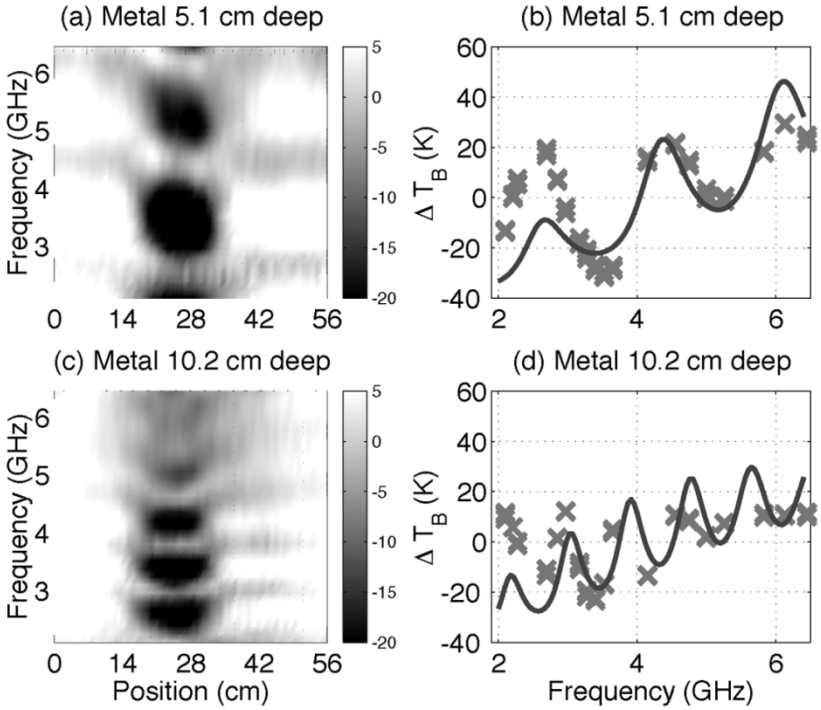

Fig. 3. Results for metal target. (a) 5.1-cm deep brightness scan, (b) 5.1-cm deep comparison of measurement and model, (c) 10.2-cm deep brightness scan, and (d) 10.2-cm deep comparison of measurement and model.

channels is maintained. Results in Section IV will show that the procedure is sufficiently accurate to allow brightness temperature oscillations in frequency to be observed.

A final issue involves the contributions of background noise sources, such as buildings, trees, and other objects. In the experiment performed, the horizon was clear in the "specular" direction for angles greater than approximately 10° above the horizon, but buildings and other sources were present in the "backward" direction. Background noise sources can corrupt measured data either by entering through antenna "sidelobes" (i.e., portions of the antenna "pattern" not observing the desired region), or by reflecting off the region under observation. Both of these contributions can vary as the antenna is translated horizontally, making their removal difficult. Observations of large metallic plates laid on the ground surface showed significant variations with position, but separating sidelobe and reflected contributions was not directly possible. Because these sources would also be present in practical application of a radiometer demining sensor, extensive efforts were not made to estimate and remove background contributions. Results will show that the oscillatory patterns due to a subsurface object remain discernible even when these effects are present. Peichl *et al.* [10] describe a system that includes both upward- and downward -looking antennas so that some background contributions can be removed; the utility of this process with the MFRAD system remains to be explored.

The contributions of background sources, potential inaccuracies in the calibration loads, and variations in received power with distance from the antenna make determination of the absolute accuracy of the measurements presented difficult. Comparisons with the three-layer model in Section IV will show differences on the order of tens of Kelvin in some cases, although the three-layer model cannot be regarded as a complete model of the experiment performed. However, the purpose of this set of measurements again is to illustrate the oscillatory brightness temperature behaviors versus frequency observed for varying target types with a semi-practical demining sensor, and not to provide precise brightness temperature values. Results will be shown to be of sufficient accuracy to meet this goal. Further experiments are in progress to quantify the experimental accuracy in more detail.

IV. Results

To illustrate horizontally scanned MFRAD data, two-dimensional images can be plotted with scan position on one axis and frequency on the other. To improve the appearance for the nonuniformly spaced MFRAD channel frequencies, a spline interpolation algorithm was used to produce a uniformly sampled frequency grid with 32 points between 2100 and 6450 MHz. Grayscale images of the resulting brightness temperatures are plotted in Fig. 3 for the metal plate target at depths of 5.1 cm [Fig. 3(a)] and 10.2 cm [Fig. 3(c)]. Contrast in these images was enhanced by subtracting the brightness scan average for each frequency; the bar in the plots indicates the color scale used for the plots in Kelvin. A bilinear interpolation was also applied to the discretely sampled image data to improve image appearance. The center of the target was located at approximately position 25 cm, varying slightly through the series of experiments.

Results clearly illustrate strong contrasts for both targets, and an oscillatory pattern in frequency that is not significant in the absence of the target. Note the small residual oscillations that are observed outside the target region are due to the subtraction

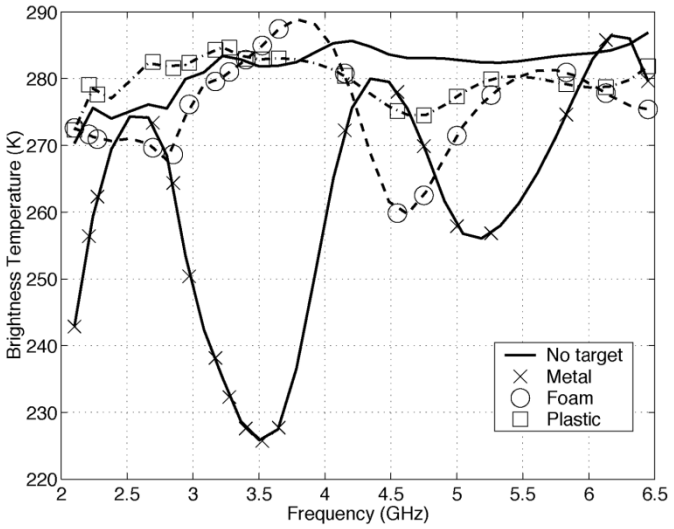

Fig. 4. Brightness temperatures versus frequency for 5.1-cm-depth metal, styrofoam, and plastic targets, along with no-target case.

of the average over position. The deeper plate is observed to produce a slightly wider response versus position, due to the larger spot size produced by the antenna at the greater depth. A more rapid oscillation in frequency for the deeper target is also obtained, as would be predicted by a layered-medium model.

Fig. 4 plots the brightness temperature versus frequency with the antenna located over the metal target center. Included in this plot are curves in the absence of the target and the corresponding styrofoam and plastic target results (discussed later). All targets are at 5.1-cm depth in the results plotted, and the symbols on the continuous (spline-generated) curves indicate the location of the MFRAD channels. The metallic target in Fig. 4 is found to produce an extremely large, oscillatory contrast from the no-target case, up to approximately 60 K in some cases. Results for the styrofoam and plastic targets show smaller contrasts, but again illustrate stronger oscillatory features than those observed in the absence of a subsurface target. The no-target case shows moderate variations in frequency with minimal oscillatory features; the variations in frequency that are observed are somewhat larger than would be expected for a homogeneous sand medium, and likely include calibration and background noise source effects. Removal of these effects remains difficult and is complicated by the fact that ground brightness temperatures in the absence of a subsurface target were found to vary up to ± 8 K as a function of antenna position. However, the stronger oscillatory features with subsurface targets still provide an important change from the no-target case, even in the presence of these complicating factors. A direct advantage of a multifrequency radiometer is clear from these plots, since a single-frequency radiometer could potentially operate on a minimum contrast point in the oscillation over frequency for the nonmetallic targets, and thereby fail in detection.

To further explore these results, Fig. 3(b) and (d) compares brightnesses versus frequency for the 5.1-cm and 10.2-cm-depth metal targets with predictions of a three-layer model (air–soil–target–soil regions), which describes observation in the far-field with an ideal antenna. The three-layer model used assumed a uniform 307-K medium temperature versus depth (measured at the sand surface in the experiment). The soil was modeled as a homogeneous sand medium, with a dielectric constant determined by the empirical model of [23] as a function of the soil volumetric moisture content. The beam fill factor was also included to account for finite target size effects: modeled target minus no-target contrasts were multiplied by this factor. Tests using data from the metallic, styrofoam (modeled as unity dielectric constant) and plastic (known to have dielectric constant 2.2) cases were performed, and the tests showed a volumetric soil moisture content of 1.75%, and beam fill factors of 33%, 33%, and 24% for the 2.5-, 5.1-, and 10.2-cm-depth targets, respectively, in the model provided a reasonable level of agreement for the multiple cases considered. These values are not unreasonable for the experimental configuration used. The resulting soil dielectric constant varies from $2.95 + j0.05$ to $2.99 + j0.14$ in the frequency range of interest. To reduce offset effects in the comparison further, the average over frequency for both the measured and modeled data is subtracted. Measured data are included for three antenna positions around the center of the subsurface target. Note the "ground truth" data used here (soil moisture content, target size and depth, beam fill factor) are needed only for comparison with the three-layer model and would not necessarily be required in a target detection procedure.

The measured data in Fig. 3 again confirm the large contrasts that are obtained in the presence of subsurface metallic targets, with a somewhat reduced contrast for the deeper target. The modeled results reproduce the measured oscillatory patterns reasonably well, although differences in amplitudes are observed particularly at the lower frequencies. Again, the purpose of these comparisons is not to produce a highly accurate model of this particular measurement (given the simple layered medium model applied), but rather to confirm that the oscillatory brightness patterns versus frequency measured by the rod antenna MFRAD system are consistent with interference patterns that could be generated in the far field by an identical but horizontally infinite subsurface object.

Fig. 5 illustrates the brightness scan data for the styrofoam block target at depths of 5.1 cm [Fig. 5(a)] and 10.2 cm [Fig. 5(c)]. The contrast is reduced compared to the metal target example, as indicated in the color scale of the plots, but the target is still observable. Oscillatory features that become more rapid with increasing target depth are observed as well. Fig. 5(c) and (d) presents comparisons with the three-layer model and again shows reasonable agreement between the measured and modeled frequency dependencies. The more complex dependence on frequency is due to interference phenomena that can result between the top and bottom interfaces of the target; in particular, the features near 3.1 GHz occur where the target is approximately one-half wavelength thick. Note the agreement is degraded at the higher frequencies for the deeper target (as in Fig. 3), indicating that the soil permittivity model used may be less realistic for the imaginary part of the dielectric constant at higher frequencies in this sand.

The plastic target presents the greatest challenge in this environment for both GPR and radiometer sensors: plastic target scanned brightnesses are plotted in Fig. 6 for targets at depths of 2.5 cm [Fig. 6(a)] and 5.1 cm [Fig. 6(c)]. A further reduction in

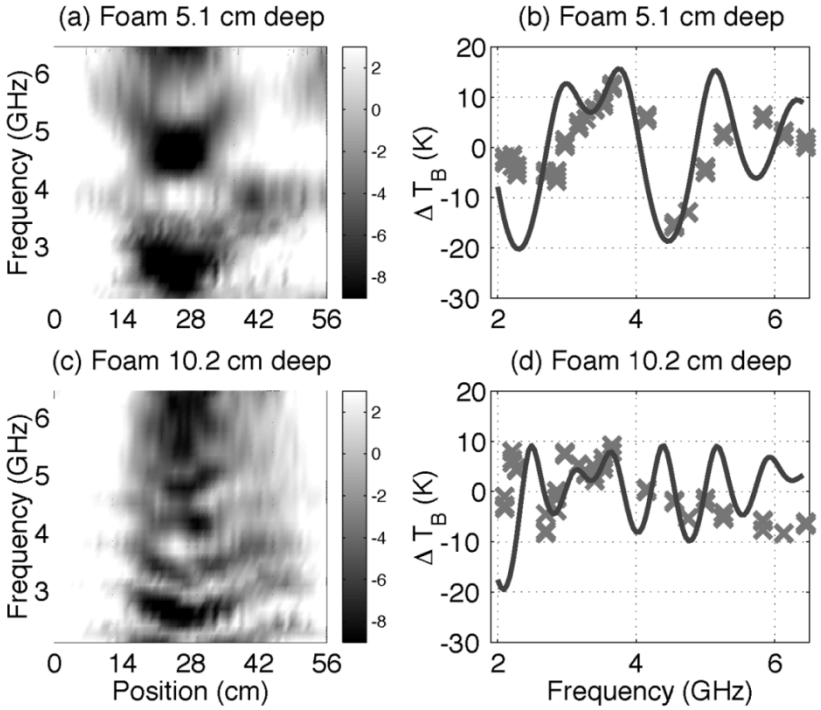

Fig. 5. Same as Fig. 3, but for styrofoam target.

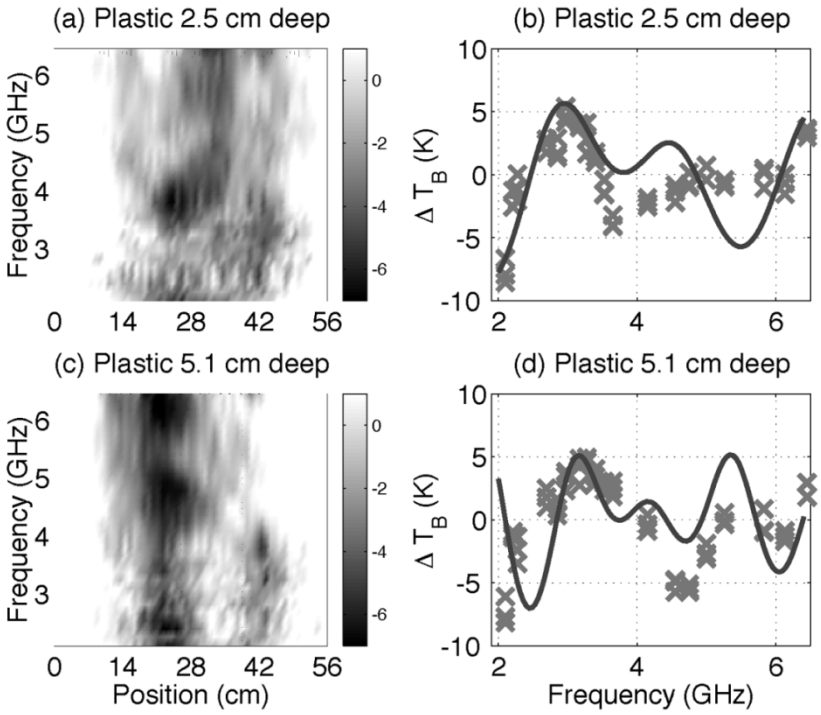

Fig. 6. Same as Fig. 3, but for plastic target at depths 2.5 and 5.1 cm.

brightness variations is observed due to the similar values of the plastic (2.2) and soil (≈ 2.97) dielectric constants. The target remains visible in the images as the generally smaller brightness values in the position 20–30-cm range, but some clutter features with similar properties (but not similar oscillatory behaviors in frequency) are also observed around positions 40–50 cm. Comparisons with the three-layer model in Fig. 6(b) and (d) show contrasts only on the level of ± 10 K, similar to the level of variation observed with position in the absence of a target. Again a somewhat complex variation with frequency is observed, with a reduced frequency variation in the modeled data around 4 GHz where the target is one-half wavelength thick. Overall, the oscillatory features remain reasonably well matched by the three-layer model, suggesting that even small contrast targets may be detectable by a search for oscillatory features in multifrequency brightness data.

V. Conclusion and Future Work

The results of this paper provide further experimental demonstration of the use of multifrequency microwave radiometers for humanitarian demining. The results are promising in that both metallic and nonmetallic subsurface objects were clearly observed in brightness data, as were oscillatory brightness behaviors in frequency similar to those predicted by the three-layer model. These features should prove advantageous in developing detection algorithms for subsurface objects; some initial results based on a fast Fourier transform algorithm have been presented in [11] and [12]. The "signal processing gain" available through a search for oscillatory features in multifrequency brightness data may allow even low-contrast plastic targets to be detected. Experiments with MFRAD continue, with goals of refining the accuracy obtained, exploring performance in other environments, and further testing of other factors such as target rotation and surface roughness effects.

Several general issues for the use of microwave passive sensors also remain that are subjects of continuing research. RFI is clearly a major concern, in that operational environments are typically not as friendly as that used in these experiments. However, new system architectures for microwave radiometers that will allow operation even in the presence of RFI are currently under development at the ElectroScience Laboratory, and should help to reduce this problem. Passive microwave sensors are also inherently local for small mine problems, because image resolutions are entirely controlled by the antenna pattern. Antennas large enough to obtain centimeter-scale spatial resolutions from reasonable standoff distances would likely be unwieldy at the frequencies of interest. However, because local operations remain a common scenario for humanitarian demining, the results of this paper provide evidence that further exploration of microwave radiometry for demining is warranted.

Acknowledgment

The assistance of F. Solheim, V. Leuski, and V. Irisov of Radiometrics Corporation is greatly appreciated. C.-C. Chen, D. Burnside, and J. Moncrief are also acknowledged for assistance with the experiments of this paper.

References

[1] L. Yuriji, B. Hauss, and M. Shoucri, "Microwave/millimeter wave radiometric detection of metal and plastic mines," *Detection and Remediation Technologies for Mines and Minelike Targets II, Proc. SPIE*, vol. 3079, pp. 652–658, 1997.

[2] R. Tan, R. Bender, and S. Stratton, "Synthetic aperture interferometric microwave radiometry for remote sensing of mines," *Detection and Remediation Technologies for Mines and Minelike Targets IV, Proc. SPIE*, vol. 3710, pp. 1003–1014, 1999.

[3] G. De Amici, B. Hauss, and L. Yujiri, "Detection of landmines via a passive microwave radiometer," *Detection and Remediation Technologies for Mines and Minelike Targets IV, Proc. SPIE*, vol. 3710, pp. 716–724, 1999.

[4] G. De Amici, A. Valles, L. Yujiri, J. Huynh, and K. Sherbondy, "Results from field tests of a passive microwave radiometer mine detector," *Detection and Remediation Technologies for Mines and Minelike Targets V, Proc. SPIE*, vol. 4038, pp. 262–269, 2000.

[5] A. Calhoun, D. Heberlein, E. Rosen, and K. Sherbondy, "Assessment of a passive microwave sensor for detecting land mines," *Detection and Remediation Technologies for Mines and Minelike Targets V, Proc. SPIE*, vol. 4038, pp. 277–285, 2000.

[6] J. T. Johnson, "Theoretical study of microwave radiometry for buried object detection," *Detection and Remediation Technologies for Mines and Minelike Targets V, Proc. SPIE*, vol. 4038, pp. 286–299, 2000.

[7] ——, "Thermal emission from a layered medium bounded by a slightly rough interface," *IEEE Trans. Geosci. Remote Sensing*, vol. 39, pp. 368–378, Feb. 2001.

[8] J. T. Johnson, B. U. Ungan, and D. R. Wiggins, "Environmental and target influences on microwave radiometers for landmine detection," *Detection and Remediation Technologies for Mines and Minelike Targets VI, Proc. SPIE*, vol. 4394, pp. 440–448, 2001.

[9] B. U. Ungan and J. T. Johnson, "A study of microwave thermal emission from a sub-surface object," *Microwave Opt. Technol. Lett.*, vol. 33, pp. 9–12, 2002.

[10] M. Peichl, S. Schulteis, S. Dill, and H. Suess, "Application of microwave radiometry for buried landmine detection," in *Conf. Proc URSI Symp. Propagation and Remote Sensing*, Garmisch-Partenkirchen, Germany, 2002.

[11] M. Peichl, S. Dill, and H. Suess, "Detection of anti-personnel landmines using passive remote sensing techniques," in *Conf. Proc. ITG/GMA-Fachtagung zu Sensoren und Mess-Systeme 2002, ITG-VDE*, Ludwigsburg, Germany, Mar. 2002.

[12] J. T. Johnson, H. Kim, D. R. Wiggins, and Y. Cheon, "Microwave radiometry for humanitarian demining: Experimental results," *Detection and Remediation Technologies for Mines and Minelike Targets VII, Proc. SPIE*, 2002.

[13] L. Yujiri, B. Hauss, and M. Shoucri, "Passive millimeter wave sensors for detection of buried mines," *Detection and Remediation Technologies for Mines and Minelike Targets, Proc. SPIE*, vol. 2496, pp. 2–6, 1995.

[14] L. Yujiri, S. Fornaca, B. Hauss, M. Shoucri, and S. Talmadge, "Detection of metal and plastic mines using passive millimeter waves," *Detection and Remediation Technologies for Mines and Minelike Targets, Proc. SPIE*, vol. 2765, pp. 330–336, 1996.

[15] J. Groot, R. Dekker, and L. van Ewijk, "Landmine detection with an imaging 94 GHz radiometer," *Detection and Remediation Technologies for Mines and Minelike Targets, Proc. SPIE*, vol. 2765, pp. 337–347, 1996.

[16] B. Blume, A. Resnick, J. Foster, J. Albers, N. Witherspoon, and J. Holloway, "PMMW data collection results," *Detection and Remediation Technologies for Mines and Minelike Targets III, Proc. SPIE*, vol. 3392, pp. 167–173, 1998.

[17] C. D. Wende, "NASA remote sensing and frequency issues," in *Proc. IGARSS*, vol. 6, 2000, pp. 2447–2451.

[18] C. C. Chen, "Novel wide-bandwidth dielectric rod antenna for detecting anti-personnel mines," in *Proc. IGARSS*, vol. 5, 2000, pp. 2356–2358.

[19] C. C. Chen, K. R. Rao, and R. Lee, "A tapered-permittivity rod antenna for ground penetrating radar applications," *J. Appl. Geophy.*, vol. 47, pp. 309–316, 2001.

[20] ——, "A ultra-wide bandwidth dielectric rod antenna for ground penetrating radar applications," *IEEE Trans. Antennas Propagat.*, 2002, to be published.

[21] W. N. Hardy, "Precision temperature reference for microwave radiometry," *IEEE Trans. Microwave Theory Tech.*, vol. MTT-21, pp. 149–150, 1973.

[22] J. Delahaye, P. Gole, and P. Waldteufel, "Calibration error of L-band sky-looking ground-based radiometers," *Radio Sci.*, vol. 37, pp. 11(1)–11(11), 2002.

[23] F. T. Ulaby, R. K. Moore, and A. K. Fung, *Microwave Remote Sensing: Active and Passive*. Norwood, MA: Artech House, 1986.

Joel T. Johnson (S'91–M'96) received the B.E.E. degree from the Georgia Institute of Technology, Atlanta, in 1991, and the S.M. and Ph.D. degrees from the Massachusetts Institute of Technology, Cambridge, in 1993 and 1996, respectively.

He is currently an Associate Professor in the Department of Electrical Engineering and ElectroScience Laboratory, The Ohio State University, Columbus. His research interests are in the areas of microwave remote sensing, propagation, and electromagnetic wave theory.

Dr. Johnson is a member of International Union of Radio Science (URSI) Commissions B and F, as well as a member of Tau Beta Pi, Eta Kappa Nu, and Phi Kappa Phi. He has received the 1993 Best Paper Award from the IEEE Geoscience and Remote Sensing Society, was named an Office of Naval Research Young Investigator, National Science Foundation Career awardee, and PECASE Award recipient in 1997, and was recognized by the U.S. National Committee of URSI as a Booker Fellow in 2002.

Hyunjun Kim (S'96) received the B.E. degree in electronics engineering from Chung-Ang University, Seoul, Korea, in 1991, and the M.S. and Ph.D. degrees from The Ohio State University, Columbus, in 1998 and 2002, respectively.

From 1995 to 1996, he was a Research Staff Member at Korea Telecom R&D Group, Seoul, Korea, where he was involved in measurement and analysis of an ATM network testbed. In 2002, he joined Intel Corporation, Chandler, AZ, where he is currently working on research and development as a Senior Package Design Engineer in the areas of signal integrity, I/O interconnect, and electromagnetic interference. His research interests include computational electromagnetics, microwave remote sensing, and electromagnetic modeling of high-speed electronic packaging systems.

David R. Wiggins, photograph and biography not available at the time of publication.

Yonghun Cheon received the B.S. degree from Yeungnam University, Yeungnam, Korea, and the M.S. degree from The Ohio State University, Columbus, in 1996 and 2002, respectively. He is currently purusing the Ph.D. degree in electrical engineering from The Ohio State University.

His research intetrests include random rough surface scattering and microwave remote sensing.